

# Model-agnostic Recognition of AI-Generated Text with Descriptive Complexity Measure

Ross Schmidt<sup>a</sup> and Ishanu Chattopadhyay<sup>○a</sup>

This manuscript was compiled on January 20, 2026

We introduce a model-agnostic approach for detecting LLM-generated text by estimating the entropy rate of text mapped to symbol streams over a (26+space)=27-letter alphabet, and show that long-form outputs from LLMs exhibit systematically lower entropy rates than human-authored prose. Our Nonparametric Entropy-Rate Oracle (NERO) exploits this signal to achieve competitive, training-free separation of human and AI text, without requiring model access. When substring-frequency cutoff profile for the estimator is used as input to a supervised Gaussian process classifier, NERO achieves near-perfect detection accuracy (AUC = 98.9%), providing a principled, complexity-theoretic framework for ranking generative capacity and tracking changes in LLM behavior over time.

entropy rate | AI-generated text detection | large language models | algorithmic complexity | probabilistic automata

With the rise of generative artificial intelligence (AI), particularly large language models (LLMs), reliably distinguishing human-authored prose from machine-generated text is no longer trivial (1–3). Here we test the hypothesis that long-form human- and machine-generated text differ in statistical complexity when mapped to symbol streams over a 27-character alphabet (26 letters plus space) and treated as sample paths of a stochastic process (4), whose entropy rate quantifies intrinsic complexity. Most existing detectors (5, 6) instead rely on language-model scoring (e.g., likelihood/rank statistics), supervised classifiers over stylistic representations, or compressibility proxies, and therefore depend on reference model access, training, or calibration to evolving generators.

We introduce a nonparametric, learning-free entropy-rate estimator that operates directly on text, without model access, supervision, or retraining. Used as a threshold score, the resulting Nonparametric Entropy-Rate Oracle (NERO) achieves competitive, training-free discrimination, and reveals systematically lower entropy rates in contemporary LLM outputs than in human prose under a shared symbolization. Optionally, using the estimator’s internal substring-frequency cutoff profile as features in a Gaussian process classifier yields near-perfect performance (AUC = 98.9%), surpassing model-driven baselines. Thus, NERO-estimated entropy rate functions as a model-agnostic statistic, akin to a physical quantity, for effective generative capacity, and provides a robust mechanism for AI text detection and a principled framework for ranking and tracking generative models over time.

## Results

To connect generative capacity with algorithmic complexity and then to entropy-rate of outputs, we begin by recalling the foundational concept of optimal two-part codes in algorithmic information theory (7). The Kolmogorov complexity  $K(x)$  of a string  $x$  is defined as the length of the shortest program (in a fixed universal programming language) that produces  $x$  and halts. It provides a rigorous, machine-independent measure of the information content or compressibility of a string. Instead of describing  $x$  directly, we can choose to first describe a finite set  $S$  that contains  $x$ , and then identify  $x$  within  $S$  by its index in a standard enumeration of all items in  $S$ . This leads to the two-part code representation:

$$K(x) \leq K(S) + \log |S| + O(1), \quad [1]$$

where  $K(S)$  is the complexity of describing the set  $S$ , and  $\log |S|$  is the number of bits required to identify  $x$  within  $S$ . When  $x$  is a *typical* element of  $S$ , *i.e.*, that it does not admit any significantly shorter description than most elements of  $S$ , the inequality becomes tight up to additive constants. The optimal two-part code is obtained by minimizing the sum  $K(S) + \log |S|$  over all such sets containing  $x$ , yielding a minimal sufficient statistic for the data.

Author affiliations: <sup>a</sup>University of Kentucky

RS carried out experimental runs and wrote the paper, IC conceived of research, implemented the algorithm, wrote the paper and procured support.

Authors have no competing interests.

<sup>2</sup>To whom correspondence should be addressed. E-mail: ishanu.ch@uky.edu

125 **Table 1. Cohorts and average entropy rates**

data source	mean H	median H	std. dev. H	count
GPT-3.5 (webform)	0.54	0.53	0.11	100
GPT-4o (webform)	0.62	0.63	0.09	98
GPT-4o (API)	0.64	0.66	0.09	136
Gemini (API)	0.66	0.67	0.10	987
Claude (API)	0.71	0.72	0.06	944
GPT-4.0 (webform)	0.71	0.71	0.09	41
GPT-5 (API)	0.74	0.74	0.08	197
Gutenberg project	0.77	0.78	0.12	4341
Arxiv papers	1.32	1.19	0.55	42

Now lets apply these notions to quantify the generative ability of AI agents (and humans). With each agent  $G_i$  we associate a set  $S_i$  that defines the collection of strings that the agent can possibly generate. Once  $S_i$  is fixed, we assume that the agent produces an individual output  $x \in S_i$  using a standard sampling procedure. This shared decoding mechanism implies that the conditional complexity  $K(x | S_i)$  is approximately constant across agents for typical strings. An equivalent way to view this assumption, is that agents draw from the same or similar set of possible strings, *i.e.*, if one agent can generate a particular string  $x$ , then so can the other, perhaps with different odds. Under either interpretation, the implication is that the conditional term  $K(x | S_i)$  is effectively constant across agents, and since for typical  $x$  this term satisfies  $K(x | S_i) \approx \log |S_i|$  (7), we have:

$$\log |S_1| = \log |S_2| + O(1). \quad [2]$$

Then, we have the proposition (See Methods for proof):

**Proposition 1** (Two-Part Code to Entropy). *Let  $G_1$  and  $G_2$  be two generative processes outputting strings over a finite alphabet  $x \in \mathcal{A}^n$ , each respectively associated with a set  $S_1$  and  $S_2$  of possible outputs. Assuming  $\log |S_1| = \log |S_2| + O(1)$ , the following equivalence holds:*

$$K(S_1) > K(S_2) + O(1) \Leftrightarrow \underset{x \sim G_1}{E} [K(x)] > \underset{x \sim G_2}{E} [K(x)] + O(1).$$

Additionally, if  $G_i$  are stationary, then

$$K(S_1) > K(S_2) + O(1) \implies H(G_1) > H(G_2) + o(1), \quad [3]$$

where  $H(G_i)$  is the Shannon entropy rate of generator  $G_i$ .

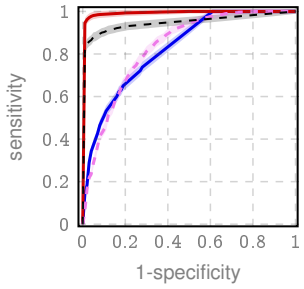
Proposition 1 motivates entropy rate as a discriminative statistic, suggesting recognition of AI-generated text by its systematically lower entropy rate. Estimating entropy rate for symbol streams is nontrivial (8). Accordingly, for NERO we adopt our prior nonparametric entropy-rate estimators based on probabilistic finite-state automata (PFSA) (9, 10) (See Supplementary Methods). With the standard approximate stationarity assumption (4) for long-form texts, Proposition 1 provides the key foundation of our claim.

## Experiments

To evaluate our claim, we use a corpus (See Table 1), comprising human-authored texts (Project Gutenberg and arXiv) and long-form outputs from contemporary LLMs (GPT-3.5, GPT-4o, GPT-4.0, Claude, Gemini, and GPT-5), using a mix of API and web-form access (See Supplementary Methods). All documents were lowercased and mapped to a 27-symbol English-plus-space alphabet, removing punctuation, digits, and non-ASCII characters. For each document we

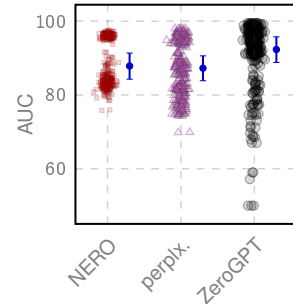
a. ROC (with 95% CI)

- NERO (no training): 82.7%
- NERO (with training): 98.9%
- - perplexity (HowGPT): 82.3%
- - - ZeroGPT: 94.9%

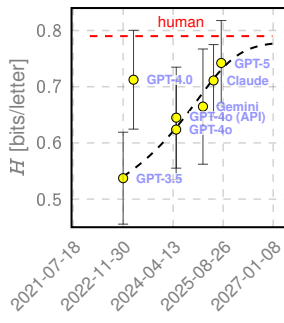


b. AUC (Cohort-Variation\*)

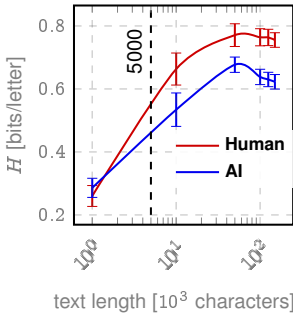
- \*381 cohort combinations
- NERO-notraining
- △ perplexity (HowGPT)
- ZeroGPT



c. Birthtime Vs Performance



d. Length dependence



e. Topic dependence in human prose (Gutenberg)

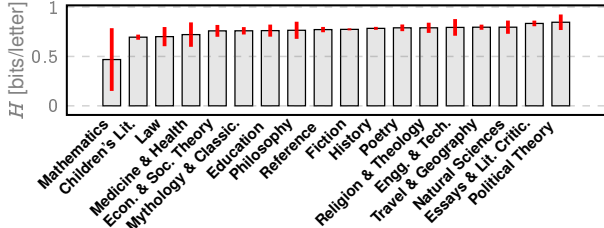


**Fig. 1. NERO performance.** a, Pooled human-AI ROC curves for training-free NERO (median entropy-rate estimate  $\hat{H}$ ), and with a Gaussian-process classifier alongside baselines (perplexity from HowGPT and ZEROGPT scoring, See Supplementary Methods). b, Cross-cohort robustness across 381 out-of-sample discrimination tasks obtained by varying the human reference set (Gutenberg, arXiv, or both) and the subset of LLM generators. c, Mean entropy rates plotted at model release dates (“birthtime”), illustrating upward drift toward the human regime; a weighted Richards fit with a fixed ceiling at the mean human rate is overlaid for descriptive smoothing. d, Entropy-rate estimates versus document length under truncation (using Gutenberg texts for humans), indicating a practical lower bound for reliable discrimination at shorter lengths around 10,000 characters. e, Genre-stratified NERO entropy rates for human prose; error bars denote 95% intervals.

compute a family of entropy-rate estimates across substring-frequency thresholds  $\{m_1, \dots, m_m\}$ , where  $m$  specifies the minimum number of occurrences required for a substring to be retained in the PFSA construction (see Methods). In the training-free setting, we use the median across thresholded  $m$ -estimates ( $H$ ). In the trained-NERO setting, the full  $m$ -dependence profile is used as features for training a Gaussian process classifier (11); importantly, the underlying entropy-rate estimator is unchanged. Using NERO, our estimates for arxiv papers ( $\approx 1.3$  bits/letter, Table 1) closely align with classic estimates of English entropy under a 27-symbol alphabet (4), whereas Gutenberg prose exhibits lower

character-level entropy, consistent with greater redundancy in narrative text. Our experimental results (Fig. 1) demonstrate:

(1) *Training-free detection.* Using  $H$  directly as a detection score yields strong LLM-human discrimination without any training. (AUC = 0.824 on the pooled evaluation, Fig. 1a).

(2) *Training using substring-frequency threshold m-dependence.* We trained a Gaussian-process classifier on the  $m$ -dependent feature vector (see Methods) using a 50/50 train-test split, improving out-of-sample discrimination to AUC = 0.989 (Fig. 1a). For comparison, the perplexity baseline (HowGPT) attains AUC = 0.830, while ZEROGPT attains AUC = 0.946 on the same pooled evaluation.

(3) *Cross-cohort robustness.* Fig. 1b reports out-of-sample AUCs for  $(2^2 - 1) \times (2^7 - 1) = 381$  distinct human-AI discrimination task obtained by varying the human reference and the subset of LLM generators included (See SI Methods). Across this combinatorial suite, training-free NERO maintains consistently strong performance, whereas trained baseline detectors exhibit substantially greater sensitivity to corpus composition and generator selection. This contrast underscores the NERO estimate as a calibration-free, model-agnostic statistic rather than a generator-dependent detector.

(4) *Temporal trajectory toward the human regime.* Fig. 1c plots cohort-level mean NERO-computed entropy rates at model release times with a weighted Richards (generalized logistic) fit and a fixed asymptotic ceiling given by the mean human rate (SI Methods), showing successive model generations shifting upward toward the human regime with diminishing returns. While not a calendar-date forecast, this supports the qualitative conclusion that model improvements are narrowing the entropy-rate gap. GPT-4.0 is a notable outlier, consistent with a regime shift induced by the architectural jump introduced in this model (multi-modal access and other experimental features) (12).

(5) *Length dependence.* Human-AI separation is robust for articles with  $> 10,000$  characters (about the length of a full-length magazine article), with loss of discrimination possibly at lengths under 5,000 characters (Fig. 1d).

(6) *Genre dependence.* Formulaic human genres (Mathematical text, Children’s Literature) attain lower entropy rates than expository genres (e.g. Literary criticism and political theory), defining the primary hard cases (Fig. 1e).

## Discussion

We show that, under shared symbolization, long-form human-authored text exhibits a consistently higher estimated entropy rate than contemporary LLMs. In the two-part code perspective, when outputs are compared within a common representation, differences in entropy rate are consistent with differences in the effective descriptive complexity of the underlying generative mechanisms, suggesting that humans might operate with a richer, more complex internal model than current AI systems.

A complementary intuition follows from *Levin’s universal semimeasure*  $m(x)$  (13), which lower-bounds the probability assignable to strings by any computable process. It defines a universal prior by summing over all prefix-free programs  $p$  (14) that produce  $x$  on a universal Turing machine  $U$  (15):

$$m(x) = \sum_{p: U(p)=x} 2^{-|p|}. \quad [4]$$

and Levin’s Coding Theorem links to Kolmogorov complexity,

$$K(x) = -\log m(x) + O(1), \quad [5]$$

which implies that strings with low  $m(x)$  are algorithmically complex and lie in the deep tails of any computable generative process. Humans operating with an internal generative model  $S_{\text{human}}$  that likely possesses significantly higher descriptive complexity than models used in AI systems, are able to generate outputs that lie deeper in the algorithmic tail of  $m(x)$ , i.e., outputs that are rarer, more contextually novel, and of higher complexity. In contrast, LLMs are trained on finite, empirical datasets where such rare strings are underrepresented (by definition of being rare); since strings with low  $m(x)$  are, by definition, uncommon, they are statistically unlikely to appear with sufficient frequency in training corpora. This possibly limits the effective model complexity  $K(S_{\text{AI}})$ , and hence constrains the AI’s ability to reproduce or extrapolate into these low-probability regions.

Thus, despite the limitations of requiring longer texts and greater computational effort, NERO yields a model-agnostic statistic that enables best-in-class detection, and principled, learning-free tracking of generative behavior over time.

## Materials and Methods

**Data acquisition.** Human-authored texts were obtained from Project Gutenberg (English-language compositions) and technical manuscripts from arXiv via the official OAI-PMH interface. AI-generated texts were produced via webform and API access to the LLMs listed in Table 1. Details on prompt design, API access, and NERO computation are provided in the Supplementary Methods.

**Code availability.** A reproducible implementation of the entropy-rate estimator and end-to-end evaluation pipeline is available under an MIT license at <https://github.com/your-repo/NERO>.

**ACKNOWLEDGMENTS.** This work was supported in part by the Defense Advanced Research Projects Agency (DARPA) under the ARC program. Views, opinions, and findings expressed are solely those of the authors.

1. Prepare for truly useful large language models. *Nat. Biomed. Eng.* **7**, 85–86 (2023).
2. E Crothers, N Japkowicz, HL Viktor, Machine-generated text: A comprehensive survey of threat models and detection methods. *IEEE Access* (2023).
3. AJ Thirunavukarasu, et al., Large language models in medicine. *Nat. medicine* **29**, 1930–1940 (2023).
4. TM Cover, RC King, A convergent gambling estimate of the entropy of english. *IEEE Transactions on Inf. Theory* (1978).
5. E Mitchell, Y Lee, A Khazatsky, CD Manning, C Finn, Detectgpt: Zero-shot machine-generated text detection using probability curvature in *Proceedings of the 40th International Conference on Machine Learning (ICML)*, Proceedings of Machine Learning Research, Vol. 202, pp. 24950–24962 (2023).
6. J Su, TY Zhuo, D Wang, P Nakov, Detectllm: Leveraging log rank information for zero-shot detection of machine-generated text in *Findings of the Association for Computational Linguistics: EMNLP 2023*. (2023).
7. P Gacs, J Tromp, PMB Vitányi, Algorithmic statistics. *IEEE Trans. Inf. Theory* **47**, 2443–2463 (2001).
8. P Grassberger, Estimating the information content of symbol sequences and efficient codes. *IEEE Transactions on Inf. Theory* **35**, 669–675 (1989).
9. I Chattopadhyay, H Lipson, Computing Entropy Rate Of Symbol Sources & A Distribution-free Limit Theorem. *ArXiv e-prints* 1401.0711 (2014).
10. I Chattopadhyay, H Lipson, Abductive learning of quantized stochastic processes with probabilistic finite automata. *Philos Trans A* **371**, 20110543 (2013).
11. CK Williams, CE Rasmussen, *Gaussian processes for machine learning*. (MIT press Cambridge, MA) Vol. 2, (2006).
12. OpenAI, Gpt-4 technical report (2023).
13. LA Levin, Laws of information conservation (non-growth) and aspects of the foundation of probability theory. *Probl. Inf. Transm.* **10**, 206–210 (1974) Originally in Russian.
14. M Li, PMB Vitányi, *An Introduction to Kolmogorov Complexity and Its Applications*. (Springer, New York, NY), 3rd edition, (2008).
15. GJ Chaitin, A theory of program size formally identical to information theory. *J. ACM* **22**, 329–340 (1975).
16. Y Horibe, A note on kolmogorov complexity and entropy. *Appl. Math. Lett.* **16**, 1129 – 1130 (2003).

## Supplementary Methods

### Proof of Proposition 1.

*Proof.* For typical  $x \sim G_i$  (7, 14),

$$K(x) = K(S_i) + \log |S_i| + O(1). \quad [6]$$

Taking expectations over  $x \sim G_i$ , we have

$$\mathbb{E}_{x \sim G_i}[K(x)] = K(S_i) + \log |S_i| + O(1). \quad [7]$$

Subtracting, we find

$$\begin{aligned} & \mathbb{E}_{x \sim G_1}[K(x)] - \mathbb{E}_{x \sim G_2}[K(x)] \\ &= K(S_1) - K(S_2) + \log |S_1| - \log |S_2| + O(1). \end{aligned} \quad [8]$$

Invoking our assumption (Eq. Eq. (2)), this simplifies to

$$\mathbb{E}_{x \sim G_1}[K(x)] - \mathbb{E}_{x \sim G_2}[K(x)] = K(S_1) - K(S_2) + O(1).$$

This completes the first part. Noting that expected Kolmogorov complexity of strings from a stationary source satisfies (14, 16):

$$\lim_{n \rightarrow \infty} \frac{1}{n} \mathbb{E}_{x \sim G_i}[K(x)] = H(G_i). \quad [9]$$

establishes the second part.  $\square$

**Nonparametric entropy-rate estimation.** We estimate the entropy rate of a stationary ergodic symbol stream using the PFSA-based nonparametric estimator introduced by Chattopadhyay *et al.* (9, 10). Given a sequence  $s = s_1 \cdots s_n$  over a finite alphabet  $\Sigma$ , the method constructs empirical next-symbol distributions conditioned on observed substrings and identifies states of an a priori unknown underlying PFSA generator as equivalence classes of histories that lead to similar future distributions. Rare substrings are excluded via a frequency threshold  $m$ , ensuring statistical reliability without assuming a parametric model or access to the underlying generator. The entropy rate is then estimated as a weighted average of the Shannon entropies of empirical symbol-generation distributions associated with that context, with the weights inferred as observed frequencies of the classes of histories that lead to individual states. The estimator is provably consistent under stationarity and ergodicity, requires no training or reference model, and operates directly on the observed text stream. Full algorithmic details and theoretical guarantees are provided in (9, 10).

**Pseudocode and Runtime Complexity.** To enhance robustness and mitigate sensitivity to internal thresholds, we apply this estimator  $M$  times across a range of substring frequency thresholds, and report the median of the resulting entropy estimates, improving concentration guarantees (Theorem 1), with the error probability decaying exponentially in  $M$ .

Runtime complexity, including threshold-based pruning and median aggregation over  $M$  thresholds, is  $O(nM|\Sigma|)$ , where  $n$  is the length of the observed stream and  $|\Sigma|$  the alphabet size (9). Thus, for a fixed  $M$ , the estimate has input-linear runtime complexity.

---

### Algorithm 1 Robust Entropy-Rate Estimation

**Input:** Symbol stream  $x_1^n$ , alphabet  $\Sigma$ , threshold range  $\{m_1, m_2, \dots, m_M\}$   
**Output:** Robust entropy-rate estimate  $\hat{H}_n$   
**foreach**  $m \in \{m_1, m_2, \dots, m_M\}$  **do**  
  | Compute  $\hat{H}_n^{(m)}$  with Chattopadhyay (9) with threshold  $m$  (ignore substrings with  $< m$  occurrences)  
  | Compute  $\hat{H}_n \leftarrow \text{median}(\hat{H}_n^{(m_1)}, \hat{H}_n^{(m_2)}, \dots, \hat{H}_n^{(m_M)})$   
**return**  $\hat{H}_n$

---

**Theorem 1** (Robustness and Concentration of the Aggregated Entropy Estimate). *Let  $x_1^N$  be a finite realization from a stationary, ergodic stochastic process over a finite alphabet  $\Sigma$ . Let  $\hat{H}_n^{(m)}$  denote the entropy-rate estimate obtained by applying the algorithm of Chattopadhyay *et al.* (9, 10) with threshold  $m$  (substrings occurring  $< m$  times ignored). Define the aggregated estimator*

$$\hat{H}_n := \text{median}\left\{\hat{H}_n^{(m_1)}, \hat{H}_n^{(m_2)}, \dots, \hat{H}_n^{(m_M)}\right\}.$$

If the indicators  $Z_i$  defined below are independent, then

$$\mathbb{P}(|\hat{H}_n - H_\star| > \epsilon) \leq \exp\left(-2M\left(\frac{1}{2} - \delta\right)^2\right). \quad [435]$$

More generally, when the  $\hat{H}_n^{(m_i)}$  are obtained from randomly drawn length- $L$  substreams of a fixed length- $N$  text and hence may be dependent due to overlap, the same argument applies with an effective number of approximately independent draws

$$M_{\text{eff}} \asymp \frac{N}{L}, \quad [438]$$

so that

$$\mathbb{P}(|\hat{H}_n - H_\star| > \epsilon) \lesssim \exp\left(-2M_{\text{eff}}\left(\frac{1}{2} - \delta\right)^2\right). \quad [446]$$

*Proof.* It follows from Chattopadhyay *et al.* (9, 10) that for sufficiently large  $n$ , for each threshold  $m \in \{m_1, m_2, \dots, m_M\}$ ,

$$\mathbb{P}\left(|\hat{H}_n^{(m)} - H_\star| > \epsilon\right) \leq \delta, \quad [451]$$

for some fixed  $\epsilon > 0$  and  $\delta < \frac{1}{2}$ . For each  $m_i$ , define

$$Z_i = \mathbf{1}\left\{|\hat{H}_n^{(m_i)} - H_\star| > \epsilon\right\}, \quad \mathbb{E}[Z_i] \leq \delta. \quad [455]$$

The median estimator  $\hat{H}_n$  deviates by more than  $\epsilon$  only if at least half of the individual estimates do:

$$S = \sum_{i=1}^M Z_i \geq \frac{M}{2}. \quad [459]$$

If  $Z_1, \dots, Z_M$  are independent, Hoeffding's inequality yields

$$\mathbb{P}\left(S \geq \frac{M}{2}\right) \leq \exp\left(-2M\left(\frac{1}{2} - \delta\right)^2\right), \quad [464]$$

which implies the stated bound.

If instead the estimates are computed from randomly drawn length- $L$  substreams of a fixed length- $N$  text, the resulting  $Z_i$  may be dependent due to overlap. In that case, the same calculation can be interpreted in terms of an effective number of approximately independent draws  $M_{\text{eff}} \asymp N/L$  (i.e., replacing  $M$  by  $M_{\text{eff}}$ ), yielding the stated overlap-limited bound.  $\square$

**Classifier design (trained-NERO).** For each document we form a fixed-dimensional feature vector  $x \in \mathbb{R}^M$  from the PFSA entropy-rate estimator by evaluating the estimate at a prescribed set of substring-frequency cutoffs  $\{m_1, \dots, m_M\}$ . Specifically, the  $j$ th feature is the entropy-rate estimate computed using cutoff  $m_j$ , so that  $x_j = \hat{H}(m_j)$ . Missing feature values (arising when insufficient support is available at a given cutoff) are imputed with zeros using a constant-value imputer.

We evaluate several standard classifiers on these feature vectors, including random forests, extremely randomized trees, AdaBoost, gradient boosting, support vector machines (SVM), and Gaussian-process (GP) classification. Unless otherwise noted, models are fit on a random 50/50 train-test split of the pooled corpus, and performance is quantified by ROC/AUC on the held-out split. For tree-based models we use class-balanced weighting and 1000–5000 component estimators to stabilize performance; for SVM we use probabilistic calibration to obtain class probabilities.

We use GP classification as the trained-NERO readout as it yields the best performance under cross-validation. The GP classifier is implemented with an RBF kernel,  $k(x, x') = \sigma^2 \exp(-\|x - x'\|^2/(2\ell^2))$ , using the standard GaussianProcessClassifier implementation (11).

**Birthtime trajectory fitting (Fig. 1c).** To summarize how estimated entropy rate of generated text changes across successive LLM models, we fit a parametric growth curve to the model-specific time series shown in Fig. 1c. Each model is represented by a timestamp (“birthtime”) corresponding to its release date, the mean NERO

497 estimate over generated tests, and an estimated standard deviation  
498 (error bar). Birthtimes were converted to elapsed time in days  
499 relative to the earliest cohort,  $x_i = (t_i - t_0)$ , yielding observations  
( $x_i, y_i, \sigma_i$ ).

500 We fit a Richards (generalized logistic) curve with a fixed  
501 asymptotic upper bound  $U$  (corresponding to mean NERO estimate  
502 for human prose), parameterized as

$$f(x; L_0, k, x_0, \nu) = L_0 + \frac{U - L_0}{(1 + \exp\{-k(x - x_0)\})^{1/\nu}},$$

505 where  $L_0$  is the lower asymptote,  $k$  the growth rate,  $x_0$  the  
506 inflection location, and  $\nu$  the shape parameter.

507 Parameters  $\theta = (L_0, k, x_0, \nu)$  were estimated by weighted  
508 nonlinear least squares using `scipy.optimize.curve_fit` with  
509 heteroscedastic weights given by the cohort standard  
510 deviations  $\sigma_i$ . We used the initialization  $(L_0, k, x_0, \nu) =$   
511  $(\max\{0, \min_i y_i - 0.03\}, 0.006, \text{median}(x), 0.6)$  and box constraints  
512  $L_0 \in [0, \min_i y_i]$ ,  $k \in [10^{-6}, 3]$ ,  $x_0 \in [-2000, 5000]$ ,  $\nu \in$   
513  $[0.05, 5]$ . The fitted parameters and their asymptotic standard  
514 errors were obtained from the returned covariance estimate  $\widehat{\text{Cov}}(\hat{\theta})$ ,  
515 and standard chi-square diagnostics were computed from weighted  
516 residuals.

516 **Data processing.** For each corpus (human-authored and AI-  
517 generated), a structured CSV file was constructed at the document  
518 level. Each row corresponds to a single novel and contains the  
519 following fields: the entropy-rate estimate computed by NERO,  
520 the perplexity-based detector score reported by HowGPT, and the  
521 estimated percentage of AI-generated text reported by ZeroGPT.  
522 These tables form the basis for all quantitative comparisons  
523 reported in the main text and figures.

523 **Topics and text generation.** Topics used to prompt the AI models  
524 were obtained from a publicly available repository of narrative  
525 prompts (<https://www.plot-generator.org.uk/story-ideas/>). The precise  
526 semantic content of individual prompts is not critical for long-form  
527 text generation; rather, it is sufficient that prompts span a broad  
528 range of genres to avoid systematic topical bias. All topics were  
529 stored in a JSON file and loaded programmatically during text  
530 generation.

530 Each AI model was prompted with the identical ordered list  
531 of topics. Consequently, the file `{model}18.txt` contains text  
532 generated from the 18th topic in the shared topic list, independent  
533 of the model used. This design ensures that differences in estimated  
534 entropy rate across models are not attributable to differences in  
535 prompt content.

535 **AI text generation prompts.** All AI-generated novels were produced  
536 using a fixed prompting protocol designed to elicit long-form  
537 narrative prose while minimizing structural or stylistic constraints  
538 beyond those necessary for length control and coherence. Identical  
539 prompt templates were used across models. Text generation was  
540 performed either via official REST APIs or, in some cases, via  
541 the OpenAI web interface using the same prompts and default  
542 generation settings; no prompt content differed between access  
543 modes.

544 **Initial generation prompt.** Each novel was initiated using the  
545 following base prompt, with bracketed fields instantiated program-  
546 matically:

547 I want you to act as a novelist writing about {topic}. The  
548 total length of the novel is about {novel\_desired\_length}  
549 characters. After generating each section of the novel, I will  
550 tell you how much text you have generated so far. In the  
551 novel, include plot development, characters, dialogue, and  
552 an overall narrative arc. Generate only the text of the novel  
553 itself, without annotations, explanations, or commentary.  
554 Write in full paragraphs and chapters of approximately  
555 {chapter\_length} characters. Continue generating Chapter 1  
556 until I tell you to stop. Generate exclusively novel text,  
557 with no metadata, confirmations, or chapter labels.

558 **Continuation prompt.** To extend generation beyond the initial  
559 context window and reach the target length, generation proceeded  
560 iteratively using a continuation prompt. At each step, previously  
561 generated text (truncated as necessary) was prepended, followed  
562 by the continuation instruction:

563 {previous generated text}

564 Here is the text generated so far. You have generated  
565 approximately {novel\_current\_length} characters. Continue  
566 writing Chapter {current\_chapter} of the novel. Maintain  
567 narrative continuity and write in complete paragraphs.  
568 Do not generate annotations, explanations, summaries, or  
569 metadata. Generate exclusively novel text.

570 **AI text generation implementation details.** AI-generated novels  
571 were produced using an automated, iterative prompting pipeline  
572 implemented in Python. Each novel was generated toward a  
573 target length of 150,000 characters using repeated completion  
574 calls under default model parameters; no temperature, nucleus  
575 sampling, or penalty parameters were explicitly set. Only the  
576 maximum completion length was controlled.

577 Chapter indices were inferred implicitly as  $[L/\ell] + 1$ , where  $L$   
578 is the cumulative character length generated so far and  $\ell = 15,000$   
579 is the nominal chapter length. Chapters were not explicitly labeled  
580 in the generated text.

581 To support long-form generation within finite model context  
582 windows, a sliding-window strategy was employed. When the  
583 concatenated prompt exceeded the available context length, only  
584 the most recent suffix of the previously generated text was  
585 retained, ensuring that the prompt plus maximum completion  
586 length remained within the model’s context window.

587 Generation continued until the target length was reached or  
588 until the model declined to continue. Responses yielding fewer  
589 than 200 output tokens were treated as refusals; in such cases, all  
590 text associated with that generation attempt was discarded and  
591 excluded from analysis.

592 API usage was subject to rate limits on requests per minute  
593 and token throughput. When limits were exceeded, generation  
594 was paused briefly before resuming. For each novel, all raw API  
595 responses and the cumulative generated text were stored in per-  
596 document metadata files to enable reproducibility and auditability.

597 The full generation pipelines are implemented in the following  
598 notebooks:

```
599 gemini:  
600 nero-data/api_data_collection/gemini_2.5_pro/get_novels.ipynb  
601 gpt4o:  
602 nero-data/api_data_collection/openai/gpt4o/get_novels.ipynb  
603 gpt5:  
604 nero-data/api_data_collection/openai/gpt5/get_novels.ipynb  
605 claude:  
606 nero-data/api_data_collection/clause_sonnet_4/get_novels.ipynb
```

607 **Human-authored text corpus.** Human-authored novels were re-  
608 trived from the Project Gutenberg corpus ([https://gutenberg.org/](https://gutenberg.org/cache/epub/feeds/)  
609 cache/epub/feeds/), which provides full-text documents together  
610 with structured metadata. All available text and metadata files  
611 were downloaded, and only English-language works were retained  
612 based on metadata fields. Legal headers and boilerplate text  
613 were removed using the `gutenbergpy` library. Novels shorter than  
614 150,000 characters after preprocessing were excluded to ensure  
615 sufficient length for stable entropy-rate estimation.

616 Technical manuscripts were collected from arXiv via the official  
617 OAI-PMH interface and converted from `.tex` source to plain text.  
618 These texts were used as a distinct human-authored reference  
619 corpus.

620 **LLM access.** AI-generated novels were produced using REST API  
621 access or web-interface access to the following models and versions:

- 622 • **Gemini:** `gemini-2.5-pro`, accessed between October 8, 2025  
623 and October 16, 2025.
- 624 • **Claude:** `claude-sonnet-4-20250514`, accessed between Au-  
625 gust 26, 2025 and September 22, 2025.
- 626 • **GPT-4o:** `gpt-4o-2024-08-06`, accessed between Novem-  
627 ber 13, 2025 and November 14, 2025.
- 628 • **GPT-5:** `gpt-5-2025-08-07`, accessed between Octo-  
629 ber 26, 2025 and November 8, 2025.

630 **Baseline detectors.** For baseline detector comparisons, the central  
631 15,000 characters of each novel were extracted and submitted  
632 to two deployed detection tools: HowGPT and ZeroGPT. The

621	central segment was used to avoid residual legal headers in human-	683
622	authored texts; the same procedure was applied to AI-generated	684
623	texts to maintain parity. HowGPT/ZeroGPT were queried on	685
624	fixed-length segments due to interface constraints. NERO was	686
625	evaluated on full texts to reflect the intended long-form detection	687
	regime.	
626	The HowGPT ( <a href="https://howkgpt.nyuad.nyu.edu/">https://howkgpt.nyuad.nyu.edu/</a> ) and the ZeroGPT	688
627	detectors ( <a href="https://www.zerogpt.com/">https://www.zerogpt.com/</a> ) were accessed between Novem-	689
628	ber 2, 2025 and November 25, 2025, with access dates varying by	690
629	model cohort. From these tools, the reported perplexity-based	691
630	detector score (HowGPT) and the estimated percentage of AI-	692
	generated text (ZeroGPT) were recorded.	
631	<b>Perplexity baseline (HowGPT).</b> The perplexity-based baseline was	693
632	implemented using the HowGPT framework, which computes	694
633	token-level likelihood statistics under a reference language model	695
634	and aggregates them into a scalar detector score. We use the	696
635	reported detector score directly rather than raw perplexity values.	697
636		698
637		699
638		700
639		701
640		702
641		703
642		704
643		705
644		706
645		707
646		708
647		709
648		710
649		711
650		712
651		713
652		714
653		715
654		716
655		717
656		718
657		719
658		720
659		721
660		722
661		723
662		724
663		725
664		726
665		727
666		728
667		729
668		730
669		731
670		732
671		733
672		734
673		735
674		736
675		737
676		738
677		739
678		740
679		741
680		742
681		743
682		744